

Waste Water Recovery Using Infrared Lamp Combined With Heated Plate

¹H. Zouaghi, ²S. Harmand, ³S. Ben Jabrallah

¹National Engineering School of Monastir, Avenue Ibn El Jazzar, 5019, Monastir, Tunisia

²University of Lille Nord, UVHC – LAMIH UMR CNRS 8201, Mont Houy, Valenciennes, Cedex 09, 59300, France

³Sciences Faculty of Bizerte – Laboratory LETTM, Zarzouna, 7021 Bizerte – Tunisia

Abstract: Animal waste presents a big problem for agricultures which have chosen to recover this waste using methanization. This may be the best solution to recover this waste and to produce another source of renewable energy. After methanization, digestate, especially pig manure, is rich in nutrients is subjected to phase separation by centrifugation. This paper addresses recovery of liquid animal wastes to use them as fertilizer and reducing the use of fossil energy.

The physico-chemical characterization of the effluent is used to justify the use of solar energy in the drying process. An experimental study of the drying kinetics of the effluent is done.

In the first part, drying using infrared radiation-based indicate that the dryer using variable temperature cycles results in the drying time reduction. In the second part, tests using heat plate were achieved. Finally we combine between infrared lamp and heat plate drying.

Results indicate that drying time is better by combining between the two modes of drying and evaporated mass flow is ameliorated. Drying time is about 4 min with an infrared temperature of 40°C and a resistor temperature of 70°C with an effluent film of 7,5 g.

Keywords Drying · infrared lamp · film · thickness · evaporated mass flow

List of symbols

<i>C/N</i>	Ratio Carbon / Nitrogen
<i>DM</i>	Dry Matter
<i>e</i>	Film thickness
<i>ICP</i>	Optical Emission Spectrometry
•	
<i>m</i>	Evaporated flow rate
<i>T</i>	Temperature
<i>UV</i>	Ultraviolet
<i>IR</i>	Infrared

Greek symbols

Φ Heat flux

Subscript

<i>f</i>	Film
<i>r</i>	Plate resistor

I. INTRODUCTION

Wastes problem have a concern for the entire population given the nuisance they cause. Studies have shown that several methods of waste recovery exist. Four major categories of treatment available to interested communities: land filling, incineration, anaerobic digestion and composting.

The choice of waste treatment type depends on several factors including the type and composition of the waste and the cost of investment.

In rural communities, it is rather waste animals, which causes a big problem on the one hand (soil pollution, rivers, ground water ...). Moreover, these discharges have a product rich in nutrients and fertilizers. Methanation presents the better solution for animal wastes in particular pig manure which is rich in nutriment. The development of biogas plants does not only reduce agricultural emissions by converting biomass but also produces thermal energy.

In France, the pig industry was concentrated in the area west of Brittany and Pays de la Loire and corresponds to 66% of the national production. Pig manure presents a source of nutrients such as nitrogen, phosphorus and potassium. It has been well established by many studies [1], [2] and [3].

After methanation, pig manure digestate has to be treated. Considering its high water content, evaporation appears the best solution for digestate. The question is whether digestate fertilizer is still of value. These analyses indicate that the rate of dry matter increases after anaerobic digestion from 8,1 to 8,9% [4] and [5].

Many studies are focalized on liquid waste recovery using evaporation.

Salihoglu *et al.*, [6] worked on sewage sludge recovery using evaporation. A solar drying plant sludge from sewage treatment was built as a tunnel-type greenhouse with a ceiling height of 2.5m. It has the principle of increasing the difference between the vapor pressure of the sludge in relation to the interior and the vapor relative pressure to obtain an efficient drying. The accumulation of the air inside the factory during the day is directed towards the rock bed for energy conservation. Lei *et al.*, [7] worked on the same type of waste. They developed a solar dryer greenhouse which was tested in the Shanghai region in China. It is characterized by a maximum radiation level of 1,002W/m² in summer. It decreases to 947W/m² in autumn and spring and it decreases to 910W/m² in winter.

The water evaporation in tanneries effluents and recovering the salt is one of the methods to use solar energy available in abundance [8], [9], [10] and [11].

Srithar *et al.*, [11] used the dryers with flat solar collectors and a sputtering evaporation system to increase the evaporation rate. In the case of plane sensor, the effluent flows over the collector. The effluent temperature and its exposure zone with the air increases, which increases the evaporation rate.

This work concerns the development of a liquid effluent by thermal evaporation. It's divided into two main parts. The first part is a physico-chemical characterization of the effluent which proves the choice of evaporation as the best waste recovery after methanation. The second part is a study of the drying kinetics of the effluent using an infrared radiation dryer. This part, concerns the combination of infrared drying with plate resistor heating.

This study will be useful for the choice of the best solar drying system and the optimization of its different parameters such as heat flux and evaporated flow rate.

II. EFFLUENT CHARACTERIZATION

To characterize the liquid effluent which presents the liquid phase of a pig manure digestate, physico-chemical tests were done. It's about a digestate having already undergone a phase separation using centrifugation. Some fertilizing elements were analyzed, as Nitrogen, Phosphorus and Potassium. The aim is to use this effluent as fertilizer on agriculture soils. Analysis results are presented in **table 1**.

Table 1: Physico-chemical characterization of the liquid effluent

Analysis	Results on raw (g/100g)	Results on dry (g/kg)
Physical analyzes		
Humidity at 105°C	97,70	-
Dry matter	2,30	-
Organic matter	1,08	468,40
Organic Carbon	0,54	234,20
pH (21°C)	8,9	-
Fertilizing elements		
C/N ratio	1,70	-
total nitrogen	0,32	138,79
Ammonia nitrogen	0,22	95,42
ureic nitrogen	< 0,10	< 43,37
organic nitrogen	0,10	43,37
phosphorus (P ₂ O ₅)	0,048	20,82
Potassium (K ₂ O)	0,61	264,56
Calcium (CaO)	0,025	10,84
Magnesium (MgO)	0,0029	1,26

The humidity and dry matter of the sample were determined using those steps. The sample is placed in an oven at temperature of 105°C until its weight become constant. The sample loses all its water content. To determine organic matter rate requires sample calcination in a furnace after determining dry matter. Mineral matter presents the difference between the total and the organic matter content. The pH is directly determined using a pH meter.

The Kjeldahl method allows for the determination of the total nitrogen. It involves blanking the liquid effluent with a concentrated sulfuric acid and a catalyst. The sample is then submitted to a gradient of temperature and mineralization. Nitrogen mineralization is achieved after distillation and trapping of the nitrogen in a solution of boric acid.

The ammonia nitrogen is given by fixing the nitrogen at low temperature. The method consists on stripping the air from the nitrogen contained in the effluent into boric acid. The nitrogen content is then determined in this acid. The determination of urea nitrogen follows the same principle. We have to measure the nitrogen content in an acid cold solution, but, in this case, the urea nitrogen content is released in the sample through using a urease enzyme.

Determining the nutrient levels (phosphorus, potassium, calcium and magnesium) was performed by extracting the liquid effluent in hot aqua regia (hydrochloric acid and concentrated nitric acid mixture) and dosing it at the ICP (optical emission

spectrometry). This metering follows the ICP measurement. It's based on the nebulization and the ionization of the liquid sample in argon plasma. The atoms contained in the sample are excited at a higher energy level. The reversion to the steady state is accompanied by a series of electromagnetic waves emission in the range of the visible and UV spectrum, which is characteristic of each element. The different wavelengths are separated using a spectrometer. The radiation intensity is proportional to concentration of the element [5].

The liquid effluent characterization indicated that its fertilizer value still high. It's favorable to be used as a fertilizer in agricultural soils.

III. EXPERIMENTAL DEVICE

The device consists on an infrared dryer related to a balance manufactured by Sartorius. The IR dryer is related to a computer which allows the measurement of the mass while changing several parameters, as temperature and drying time. (**Fig.1.a**). The balance has an accuracy 10⁻³g. The IR lamp temperature is between 40 and 160°C.

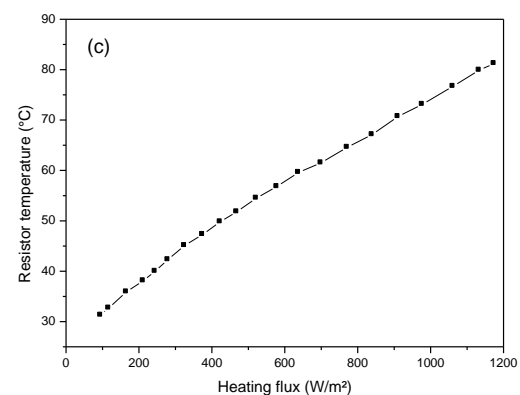
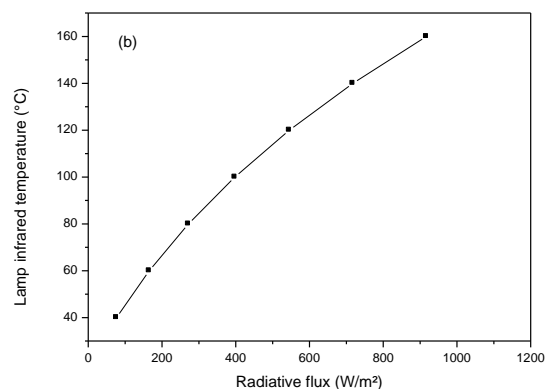
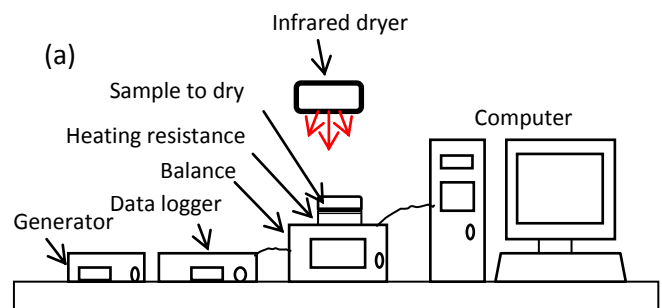


Figure 1: Evaporation test bench static film effluent: (a) Bench

test; (b) Flux curve as function of IR lamp temperature; (c) Flux curve as function of resistor temperature

Heating using a plat is contemplated using a heating resistor of 88,1Ω. It has a circular shape which radius is about 10cm. It's covered by insulating layer Bakelite having 1cm thickness. To ameliorate heat transfer, a conductive layer is made between heating resistor and sample container. A very fine thermocouple which type is K is placed between resistor and conductive layer. Its accuracy is about ±1°C.

To measure temperature, the device is connected to a data acquisition system. The radiative flux that reaches sample surface is measured using a flow meter connected to a data logger. Its uncertainty is about ±0,5mV. The variation of the radiation flux as a function of the IR lamp temperature is shown in **fig.1.b**. The radiation flux increases with an increase in the temperature of the lamp. Its maximum is about 916,9W/m² corresponding to an IR lamp temperature of 160°C.

Using a generator, heating power resistance can be determined. The heating flux presents the power per unit area. The curve of heating plate temperature as a function of radiative flux is presented in **fig.1.c**.

The curve of mass sample as function of the drying time is shown on the computer using software specialized in mass measuring.

IV. EXPERIMENTAL RESULTS

Many tests were conducted; the aim is to study the liquid effluent behavior to dry when it is at rest.

A. Effect of liquid surface to dry using constant heat flux

A Comparison is made between two samples. They are characterized by the same thickness but different surfaces while maintaining the IR lamp heat flux at 916,9W/m².

Table 2: Samples characteristics

e = 1,1 mm	Volume	Mass	Surface
<u>Config.1</u>	7,8 ml	7,110 g	71cm ²
<u>Config.2</u>	4,1 ml	3,325 g	33cm ²

When the liquid effluent is exposed to the infrared lamp radiations, its water content decreases until its mass stabilized. Drying curve passes through two phases: a phase of rapid decreasing mass and another with slow descending of the mass as it's shown in **fig.2**.

The digestate, having water content greater than 97%, evaporates. The rapid increase in the weight of the digestate can be explained by the free water contained in the liquid effluent. When the water content is between 30-40%, the sample no longer contains free water in its cavities. The remaining material is then considered saturated with bound water, which takes longer to evaporate. Therefore, there is a slow decay of the curve until it become constant [5].

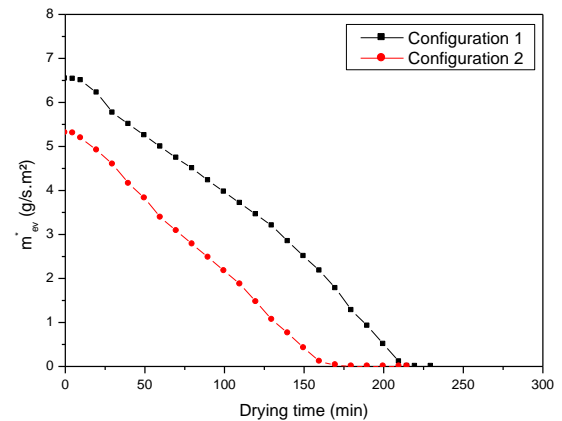
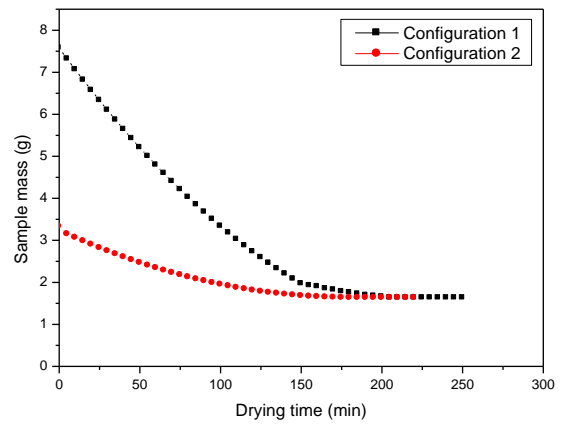


Figure 2: Drying curve depending on the given configurations

Evaporated mass flow decreases as function of time. It's maximum at t=0s. Evaporated flow rate is defined according to Fick law as the opposite of concentration gradient between water vapor in the air and that at the interface of liquid film. At t=0s, the air is supposed dry; its vapor concentration is low, so evaporated mass flow is max. During evaporation process, vapor released from the liquid makes the air more saturated, which explains the decreasing curve of evaporated mass flow.

Results show that even if the sample thickness remains constant, samples having a greater portion of water will take longer to dry. The configurations presented in **table 3** were used in drying tests at the same heat flux of 916,9W/m².

Table 3: Samples characteristics

Volume = 7,8 ml	Surface
<u>Config.1</u> : e = 1,1 mm	71cm ²
<u>Config.3</u> : e = 2,3 mm	33cm ²

Drying curves have the same shape and its drying times are very similar using configurations presented in **table 3**. A sample from configuration 3 has a drying time of 255min. This indicates that the thickness of the liquid has no influence on the drying kinetics as the drying remains a surface phenomenon.

In the rest of the work, the characteristics of **config.2** were used. The IR lamp heat flux is going to be varied.

B. Effect of the IR lamp heat flux

Using **config.2**, drying time is the lower. Tests are carried out using different infrared lamp heat flux. **Table 4** presents the drying time for each lamp heat flux.

Table 4: Characteristics of the dried samples

$\phi_{IR\ Lamp}$ (W/m ²)	76,6	271,3	545,4	916,9
Initial mass (g)	3,276	3,273	3,277	3,275
Final mass (g)	0,869	0,864	0,862	0,859
Drying time (min)	240	235	220	210

Drying curves have the same features. They have two phases: a fast phase and slow decaying phase decay (**fig.3**).

When IR heat flux is higher, drying is faster. The drying time is a minimum for 916,9W/m². At this radiative flux, the final weight was 0,867g.

Evaporated flow rate decreases as function of time. Its maximum corresponds to the higher heat flux until the drying time is about 130s. Starting at drying time between 130 and 160s, the sample having the higher heat flux corresponds to the lower evaporated flow rate.

In the following part, the aim is to minimize the drying time depending on infrared lamp radiative flux. For all heat fluxes, the phase of rapid decay is almost identical for all trials. The purpose is to decrease radiative heat flux during rapid phase and increase the lamp heat flux during the second phase until mass stabilization.

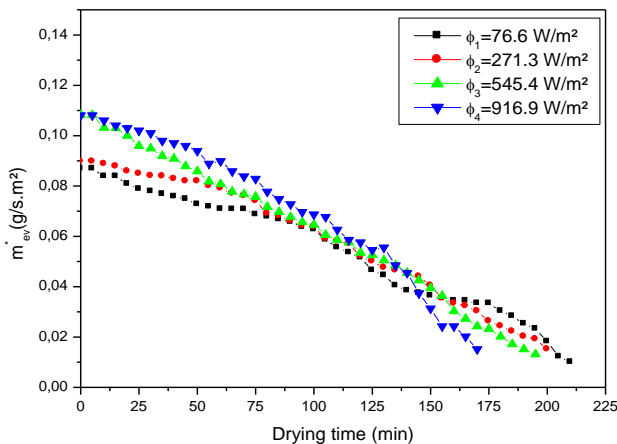
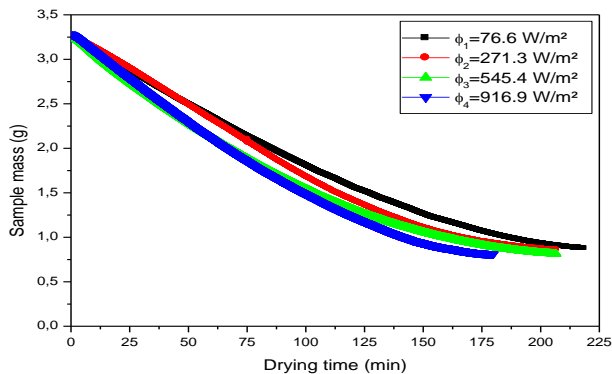


Figure 3: Drying curves for several IR lamp radiative flux

C. Variation of the lamp radiative flux during drying

The aim is to reduce radiative heat flux when evaporation rate is high and increasing the temperature during the slow decay phase.

At first, a gradual increase of heat flux using use of three heat flux ranges followed by two ranges for the two phases. **Fig.4** shows the various heat flux cycles used and the corresponding drying times.

The minimum drying time corresponds to cycle 4 (**table 5**). It's about 3h20min.

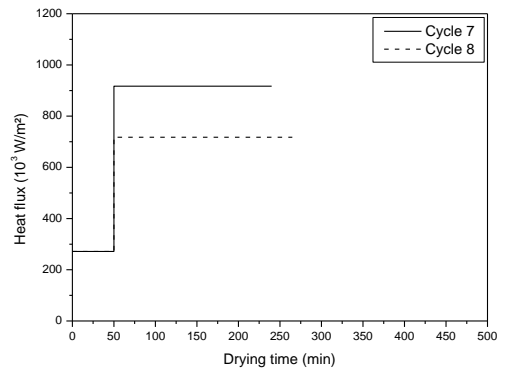
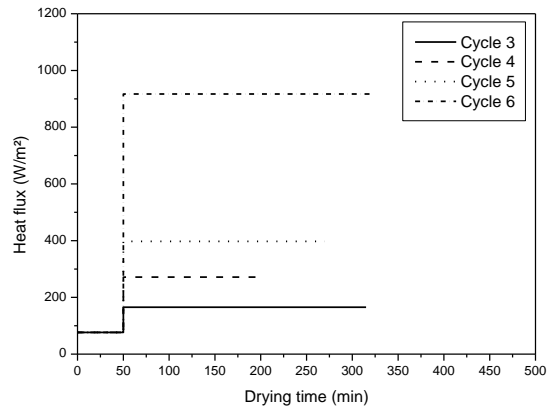
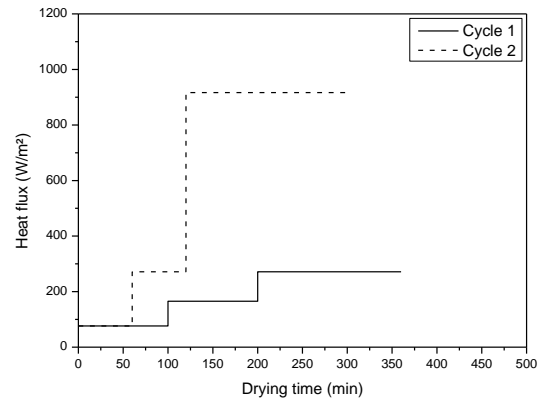


Figure 4: Distribution of IR lamp heat flux for each cycle

The study of drying kinetics of the liquid effluent at rest indicates that the overall drying time depends somewhat on the thickness of the liquid film but depends strongly on IR lamp heat flux.

Table 5: Drying time for each cycle

Cycle	Drying time (min)
1	360
2	300
3	315
4	200
5	270
6	320
7	240
8	265

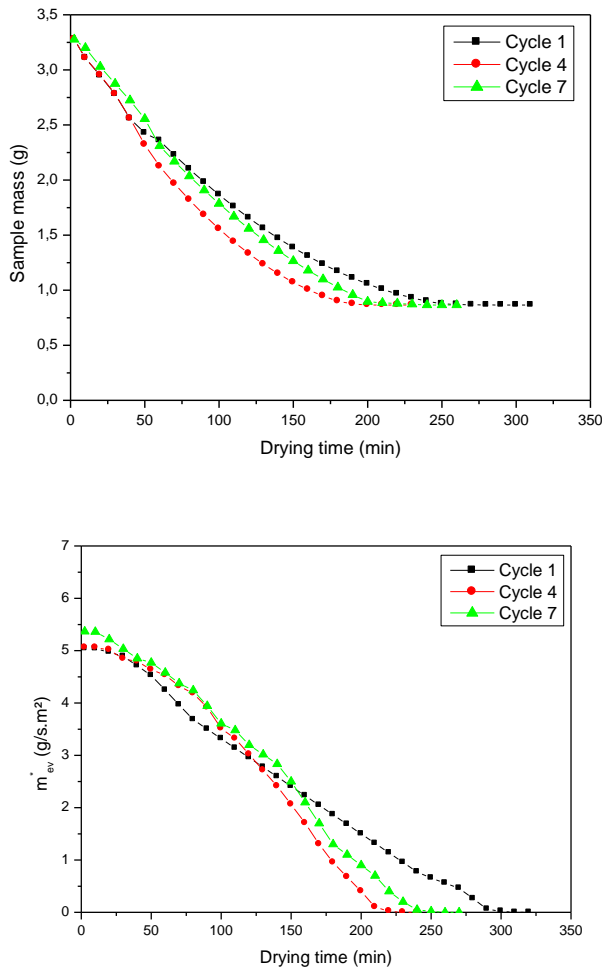


Figure 5: Drying curves for cycle 2, 4 and 7

The shortest drying time is from cycle 4, when heat flux is 315,9W/m² during 60min and 511,1W/m² until the end of drying.

The evolution of evaporated mass flow for different heat flux cycles indicates that it is decreasing.

D. Drying using heating resistor

Using sample characteristics of **config.1**, drying sample was performed for different heat flux.

Mass variation curve over time has the same shape as that of drying using IR lamp. It decreases as function of time and has two phases, a fast decay phase and another slow linked to the same phenomenon described above.

The initial average weight is of 7,572 g. After drying, the final sample mass is around 1,629 g. Results are presented in **fig.6**.

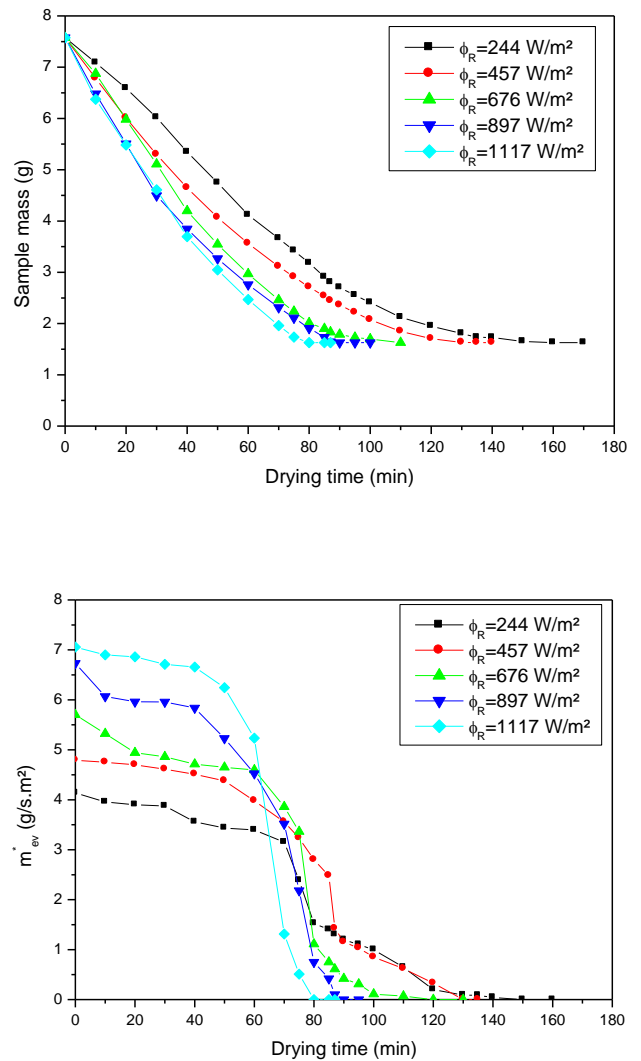


Figure 6: Drying curves for several plate heat fluxes

When plate heat flux increases, sample drying is faster. If $\Phi=244W/m^2$, sample dried after 156min. Against by, if heat flux is about 1117W/m², drying time is reduced by half, it is 76min. So, the kinetics drying is strongly related to the plate heat flux.

Evaporated mass flow decreases during time. Evaporated mass flow increases with the increase of heat flux, its maximum is about 7.1g/s.m² when heat flux is about 1117W/m² at t=0s comparing to 4,1g/s.m² when heat flux is 244W/m² at the same time. So, evaporated flow is related to heat flux when drying time doesn't reaches 70s. After that time, when heat flux is max, evaporated flow is minimum. So, they are inversely proportional.

For low heat flux (between 244 and 600W/m²), evaporated flow decreases slowly from drying time about 90s. When heat flux is high evaporated mass flow decrease is faster.

E. Combining of drying with infrared lamp and heating resistor

In this part, heating using IR lamp and heating resistor is made. Tests start by setting the IR lamp radiative flux at 76,6W/m² (40°C) and varying the plate heat flux. Before posing

sample, plate and lamp temperature have to be stabilized. Results are presented **fig.7** and its specificities are presented in **table 6**.

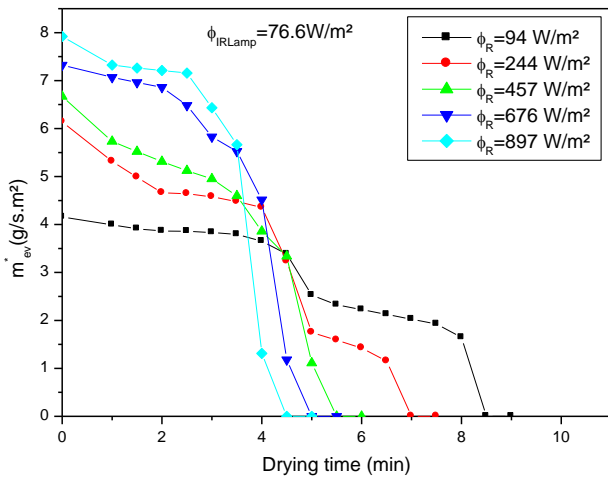
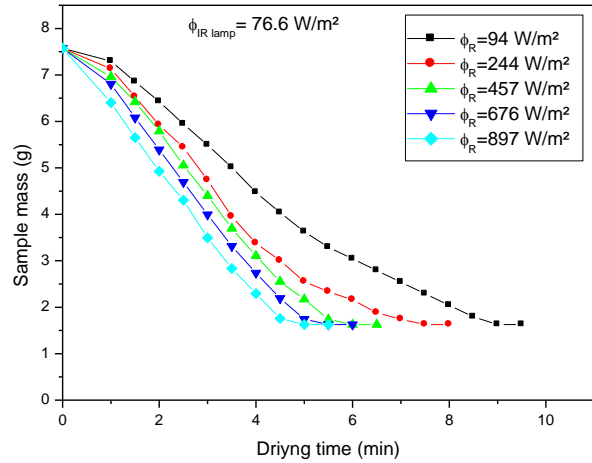


Figure 7: Drying curve for constant IR lamp flux

Fixing IR lamp radiative flux, when plate heat flux increases, the mass and evaporated flow rate decreases as function of time. The initial sample mass is about 7,573g. After drying, at the end of drying, it's about 1,627g. The shortest drying time is about 4min when the total heat flux is about 973,9W/m².

Having a stabilized IR lamp of 76,6W/m² and a resistor heat flux 897W/m², liquid temperature is about 93°C. It's favorable to have the shortest drying time of 4,4 min.

Evaporated mass flow is better by combining heat flux of resistor and infrared lamp (**Fig.8**). It increases with the increase of heat flux. The maximum is about 7,1g/s.m² and the average is about 6g/s.m² for a total heat flux of 973,9W/m².

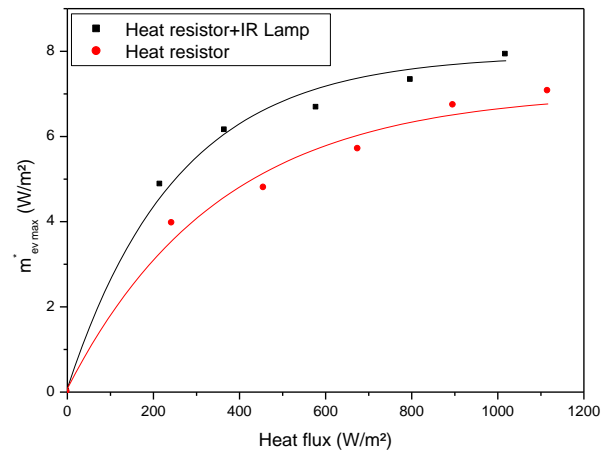
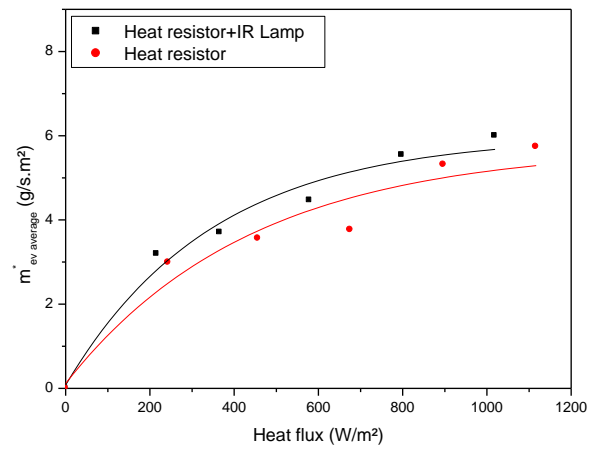
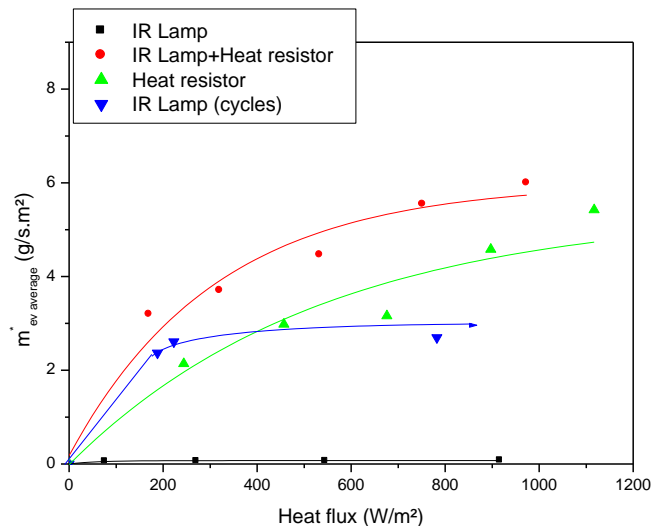


Figure 8: Average and maximum of evaporated mass flow as function of total heat flux

The increase of the evolution of evaporated mass flow according to different heating mode is presented in **fig.9**.



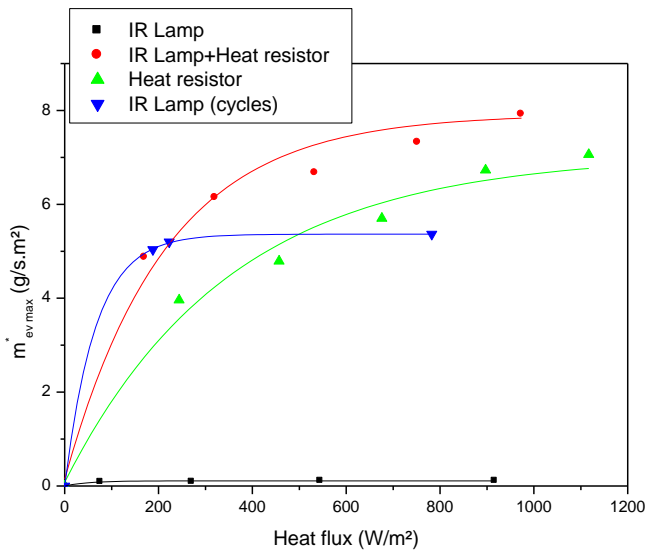


Figure 9: The maximum evaporated mass flow for different heat fluxes and heating mode

Evaporated mass flow is maximum when liquid effluent is heated using the IR lamp and heating resistor. Trying to increase evaporated mass flow, it's necessary to increase IR lamp heat flux using cycles. Evaporation phenomenon isn't observed because it will just take some seconds.

CONCLUSIONS

A study of the liquid phase behavior of pig manure digestate, which is rich in nutrients, has been established. Two heating modes were made.

Using IR lamp, digestate drying kinetics at rest indicates that this phenomenon is not dependent on the thickness of the sample but is a surface phenomenon. The optimization of the drying time doesn't only depend on the heat flux but also on heating cycles.

Using heating resistor, drying time is shorter when plate heat flux is higher. It corresponds also to the higher evaporated mass flow.

Combining heating by IR lamp and resistor, drying time is about 4min when heat flux of IR lamp is 76,6W/m² and resistor heat flux is about 897W/m². So drying is related to heat power.

This paper presents a preliminary study on liquid effluent evaporation. It allows characterizing the liquid effluent to choose the best solar evaporation model by optimizing the operating parameters of the evaporator. Heat flux of the infrared lamp corresponds to the evaporator solar flux for the evaporator. When heating by resistance can be translated by a heating system designed at the back of the inclined plate. This waste will be used as a fertilizer in agricultural soils as they are rich in nutrients.

References

[1] Levasseur P, 2010. *Déshydratation des digestats de méthanisation Analyse économique de quatre procédés*. La revue technique de l'IFIP, TechniPorc, Vol. 33, N°5, 2010.
[2] Granier R, Texier C, 1993. *Production du lisier de porc à l'engrais : quantité et qualité*. Techni-porc, mars 1993, p 23-31.

[3] Latimier P, Gallard F, Corlouër A, 1996. *Actualisation des volumes et des quantités d'azote, de phosphore et de potasse rejetés dans le lisier par un élevage naisseur-engraisseur*. Journées Rech. Porcine en France, 28 : 241-248.
[4] Levasseur P, 1998. *Composition et volume de lisier produit par le porc : Données bibliographiques*. TECHNI - Volume 21, n°4, 1998 : p 16 – 19.
[5] Zouaghi H, Harmand S, Ben Jabrallah S, 2015. *Evaporation experimental study of liquid effluent after methanation*. International journal of agriculture innovations and research. Volume 4, issue 2, p381-389.
[6] Salihoglu NK, Pinarli V, Salihoglu G, 2006. *Solar drying in sludge management in Turkey*. Received 30 April 2006; accepted 2 August 2006 Available online 17 November 2006.
[7] Lei Z, Dezhen C, Jinlong X, 2009. *Sewage sludge solar drying practise and characteristics study*. In: Proceedings of power engineering conference, IEEE.
[8] Mani, A, Srinivasa Murthy S, 1993. *Solar Evaporation Ponds for Tannery Effluent Treatment*. A Technical Report, TALCO Ltd., Chennai, India.
[9] Mani, A., Srinivasa Murthy, S., 1994. *Analysis of an open type flat plate collector for tannery effluent treatment*. Energy Conversion and Management, 35(12):1061-1071.
[10] Srithar, K., Mani, A., 2003. *Comparison between simulated and experimental performance of an open solar flat plate collector for treating tannery effluent*. International Communications in Heat and Mass Transfer, 30(4):505-514.
[11] Srithar, K., Mani, A., 2004. *Analysis of a single cover FRP flat plate collector for treating tannery effluent*. Applied Thermal Engineering, 24(5-6):873-883.